Monolithic folded resonator for evanescent wave cavity ringdown spectroscopy

Andrew C. R. Pipino

An optical resonator is characterized that employs both ultrahigh-reflective coated surfaces and total internal reflection to enable cavity ringdown spectroscopy of surfaces, films, and liquids. The monolithic folded design possesses a polarization-independent finesse that allows polarization-dependent phenomena, such as molecular orientation, to be probed. Although a restricted bandwidth (~15% of the design wavelength) results from use of reflective coatings, the resonator provides high sensitivity and facile operation. A minimum detectable absorption of 2.2×10^{-6} was obtained for single laser shots by use of multimode excitation at 530 nm with an excimer-pumped, pulsed dye laser.

OCIS codes: 230.5750, 240.6490, 300.1030.

1. Introduction

In recent years, cavity ringdown spectroscopy[1–3] (CRDS) has been applied widely for the measurement of weak optical transitions and low number densities, equaling or exceeding other optical absorption techniques in sensitivity. CRDS utilizes the intensity decay time or ringdown time of a high-finesse optical cavity as the absorption-sensitive observable. Typically, the optical cavity is constructed from two or more ultrahigh-reflective coated mirrors that have appropriate spacing and radii of curvature to form a stable resonator. A laser source excites one or more cavity modes which then decay exponentially with a ringdown time given by

$$\tau(\omega) = \frac{t_r}{\mathcal{L}_0(\omega) + \mathcal{L}_{\mathrm{abs}}(\omega)}, \tag{1}$$

where $\mathcal{L}_0(\omega)$ and $\mathcal{L}_{\mathrm{abs}}(\omega)$ are the round-trip intrinsic and absorption loss, respectively, and t_r is the round-trip time for light propagation in the cavity. Measurement of the difference in the intensity decay rate ($\propto 1/\tau$) in the presence and absence of an absorbing medium as a function of laser frequency yields the absolute absorption spectrum of the medium. The minimum detectable absorption in CRDS can be expressed[4,5] as the product of the intrinsic loss and the relative uncertainty in the ringdown time, or $(\mathcal{L}_{\mathrm{abs}})_{\mathrm{min}} = \mathcal{L}_0 * (\Delta\tau/\tau)_{\mathrm{min}}$, which separates approximately into cavity- and instrumentation-dependent terms, respectively. Optimization of sensitivity in CRDS is therefore achieved by one's minimizing the intrinsic cavity loss and measuring the ringdown time with the highest possible precision. With a few exceptions,[6–11] CRDS has been applied mainly to gas-phase diagnostics. The dependence of $(\mathcal{L}_{\mathrm{abs}})_{\mathrm{min}}$ on the intrinsic loss presents a challenge for extension of CRDS to surfaces and condensed media. New cavity designs are needed that allow other states of matter to be probed, while providing low intrinsic loss and simplicity of operation.

Evanescent-wave cavity ringdown spectroscopy (EW-CRDS)[7–9,11] combines the properties of total internal reflection (TIR), including broad bandwidth, ultrahigh reflectivity, and evanescent wave generation with CRDS, allowing sensitive condensed-matter spectroscopy. The first demonstration of EW-CRDS employed a Pellin–Broca prism in a conventional CRDS cavity.[7] Submonolayer coverage of adsorbed iodine was detected by the change in ringdown time arising from evanescent-wave absorption at a TIR surface. However, the Pellin–Broca prism provided moderate finesse only for a single polarization state, which introduced a large intrinsic loss arising from depolarization by residual birefringence and precluded the determination of molecular orientation at the surface. In addition, because conventional CRDS mirrors were used, the cavity possessed a narrow spectral bandwidth. Circumventing these limitations, a TIR ring minicavity was employed for EW-

The author is with the Chemical Science and Technology Laboratory, Process Measurements Division, National Institute of Standards and Technology, 100 Bureau Drive, Gaithersburg, Maryland 20899-8363. His e-mail address is andrew.pipino@nist.gov.

Received 20 July 1999; revised manuscript received 19 November 1999.

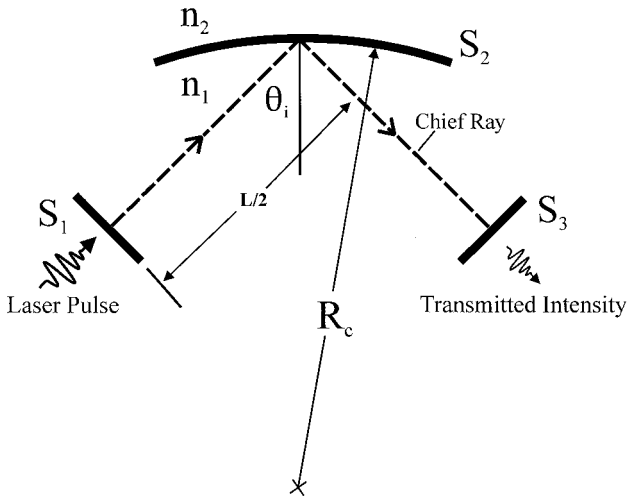

Fig. 1. Schematic diagram of a monolithic optical cavity that permits CRDS of surfaces, films, and liquids. Surfaces S_1 and S_3 of the monolithic solid are coated with an ultrahigh-reflective dielectric coating, as employed in gas-phase CRDS cavities. For $n_1 > n_2$, surface S_2 becomes a TIR mirror if $\theta_i > \theta_c = \sin^{-1}(n_2/n_1)$. The three-mirror system forms a stable optical resonator for a judicious choice of mirror separation and spherical radius of curvature R_c given by inequality (2). The evanescent wave at the TIR surface probes optical absorption of an ambient medium through a change in ringdown time of the cavity.

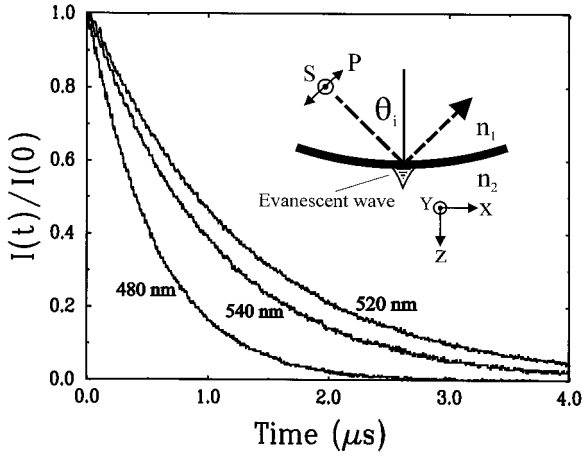

Fig. 2. Single-shot ringdown transients for three wavelengths for a fused-silica, monolithic cavity as in Fig. 1 with $L = 3.0$ cm, $R_c = 7.5$ cm, and $\theta_i = 45°$. An excimer-pumped, pulsed dye laser was employed as the excitation source. The transients were detected with a photomultiplier tube and a digital oscilloscope, which applied a 25-MHZ bandpass filter. The inset defines the in-plane (P) and out-of-plane (S) polarizations and the coordinate system at the TIR surface.

CRDS, which has a broad bandwidth and a small polarization-independent intrinsic loss.[8,9,11] However, to excite the modes of the TIR ring cavity, photon tunneling is used, which requires precise positioning of one or more coupling prisms. In the following, a new monolithic resonator design for EW-CRDS is demonstrated that employs both ultrahigh-reflective coatings and TIR. For applications that do not require a broad bandwidth, the design has several advantages, including direct excitation by a propagating wave, high finesse for both polarization states, and simplicity of operation.

2. Cavity Design and Performance

Figure 1 shows a schematic diagram of the folded resonator design, which is formed from a monolithic solid of ultralow-loss optical material having a refractive index n_1. Planar surfaces S_1 and S_3 are ultrahigh-reflective coated surfaces, whereas convex surface S_2 forms a TIR mirror if $\theta_i > \theta_c = \sin^{-1}(n_2/n_1)$, where n_2 is the refractive index of the ambient medium. The resulting twin-waist, astigmatic resonator is stable if the spherical radius of curvature R_c of S_2 and the unfolded cavity length L satisfy the condition[12]

$$0 \le \left(1 - \frac{L}{R_c \cos \theta_i}\right)^2 \le 1 \qquad (2)$$

in the tangential plane where the effective radius of curvature $R_{\text{eff}} = R_c \cos \theta_i$. Note that this condition assures stability for the sagittal plane for which $R_{\text{eff}} = R_c/\cos \theta_i$. The ringdown time for this cavity is given by Eq. (1) with intrinsic loss $\mathcal{L}_0(\omega) = 2(\mathcal{L}_c + \mathcal{L}_{\text{surf}} + \mathcal{L}_{\text{bulk}})$, where the $\mathcal{L}_i$ are the per pass coating, TIR surface scattering, and bulk loss, respectively, and $t_r = 2Ln_1/c$, where c is the speed of light in vacuum. Ideally, $\mathcal{L}_c$ should be dominated by residual transmission with a minimal contribution resulting from coating absorption and scattering. When superpolished, surface scattering losses at all reflective surfaces are minimized by a root-mean-square (rms) surface roughness of ~0.05 nm.[13] At the design wavelength of 520 nm for this research, surface scattering losses can be significant. For example, the single-surface scattering loss at 520 nm is estimated to be[8] $\sim 150 \times 10^{-6}$ for a standard laser-grade optical finish of 0.5-nm rms roughness for fused silica at $\theta_i = 45°$. Under the same conditions, a superpolished surface with 0.05-nm rms roughness will have a single-surface scattering loss of $\sim 1.5 \times 10^{-6}$. Diffraction losses can be neglected for the resonator of Fig. 1 if the resonator mode diameter is small relative to the system's clear aperture. Nonspecular transmission losses can also be neglected if $\theta_i - \theta_c \ge 1°$, depending on the curvature of the incident wave front at the TIR surface.[14] The sample absorption $\mathcal{L}_{\text{abs}}$ is probed by the evanescent wave that emanates from the apex of the TIR surface, decaying exponentially in space outside the resonator with a decay length that is comparable to the incident wavelength.[15]

Figure 2 shows single-shot ringdown transients at 480, 520, and 540 nm for a fused-silica (Amersil 311)[16] resonator as depicted in Fig. 1 with $L = 3.0 \pm 0.03$ cm, $R_c = 7.5 \pm 0.001$ cm, and $\theta_i = 45.0° \pm 0.08°$. The surface normals for S_1, S_2, and S_3 lie in the same plane to within $\pm 0.08°$. Surfaces S_1 and S_3 were coated with an ultrahigh-reflective coating centered at ~520 nm with an estimated loss of $\mathcal{L}_c = 1.2 \times 10^{-5}$

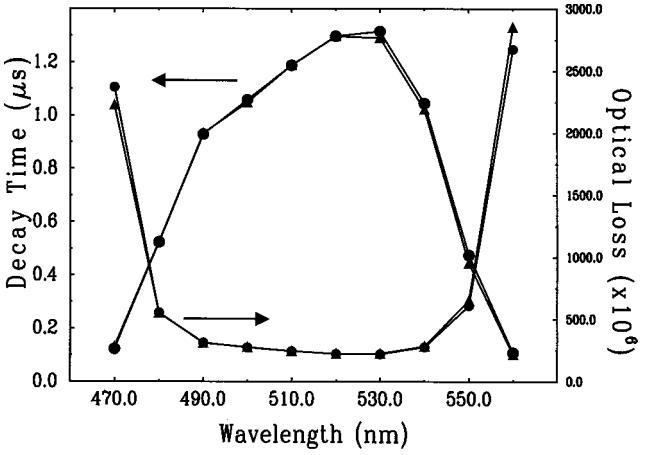

Fig. 3. Intrinsic loss and ringdown time are shown on opposite axes as a function of wavelength for the monolithic cavity. The useful bandwidth of the resonator is approximately 80 nm, limited by the coating reflectivity. A minimum loss of 220×10^{-6} occurs at 530 nm, which is determined mainly by the bulk attenuation of fused silica. The circles indicate S polarization; triangles indicate P polarization. Note that the intrinsic losses for the two polarizations are nearly equal.

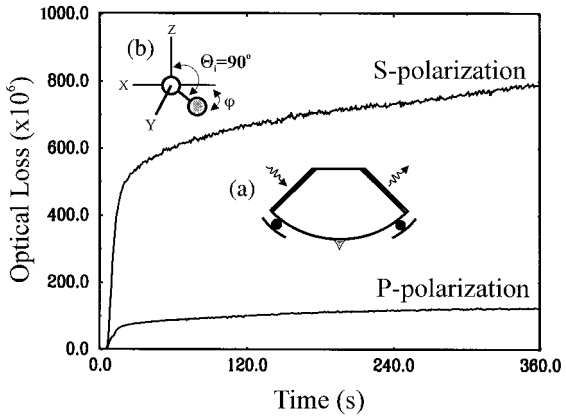

Fig. 4. Optical losses at 540 nm for S- and P-polarized cavity modes as a function of time during exposure of the TIR surface to I_2 vapor at room temperature. Inset (a) indicates the geometry for sealing the TIR surface to the I_2 source by an O ring. The S-polarized optical loss is found to be much larger than the P-polarized case. Because the electric field associated with an S-polarized mode lies entirely in the plane of the TIR surface, the ratio of absorbances suggests that surface-bound I_2 lies flat on the surface [$\Theta = 90°$ in the inset (b)] as discussed in the text.

per reflection according to the manufacturer's specifications (Research Electro-Optics, Boulder, Colorado).[16] Because the angle of incidence was selected to be close to the critical angle for a fused-silica–air interface ($\theta_c \sim 43.3°$), this particular design permits diagnostics of adsorbed layers and thin films with a significant surface electric field enhancement.[15] An excimer-pumped dye laser, which generated 20-ns, ~0.25-mJ laser pulses, was used without mode matching to generate the transients by light injection through S_1. The transmission through surface S_3 was monitored with a photomultiplier tube and an 8-bit digital oscilloscope. The resonator was mounted on a prism table with control of all degrees of freedom relative to the incident laser beam. Course alignment was accomplished by tuning the laser wavelength to the edge of the resonator bandwidth to permit visual inspection of the transmitted modes. After adjustment of the resonator orientation to obtain low-order mode excitation, the collection and detection hardware were configured, allowing final alignment by observation of ringdown transients near the design wavelength. Figure 3 shows the ringdown time and round-trip intrinsic loss on opposite axes as a function of wavelength for S and P polarizations, which are defined in the inset of Fig. 2. The useful bandwidth of the resonator can be seen to be approximately 80 nm, which is limited by transmission of the coated surfaces. Note that the intrinsic loss is essentially independent of polarization. The minimum round-trip loss of 220×10^{-6} is found for S polarization at 530 nm with $\tau_S(530\ \text{nm}) = 1.316\ \mu\text{s}$, which is bulk-loss limited. By averaging 25 individually acquired ringdown times, a relative uncertainty in τ (530 nm) of $(\Delta\tau/\tau)_{\min} = \sqrt{2}\sigma_\tau/(\tau\sqrt{N}) = 0.002$ was obtained, where σ_τ is the ensemble standard deviation and N is the number of decay times averaged. This yields a minimum detectable absorption of $(\mathcal{L}_{\text{abs}})_{\min} = \mathcal{L}_0{}^*(\Delta\tau/\tau) = 4.4 \times 10^{-7}$, corresponding to a noise equivalent absorption of $7.0 \times 10^{-7}\ \text{Hz}^{-1/2}$ for a 10-Hz repetition rate.[17]

3. Measurement of Molecular Orientation

The polarization-independent finesse of the resonator in Fig. 1 allows polarization-dependent phenomena to be probed in the evanescent wave. Because the absorbance A will be significant only when an electric field component is aligned with a molecular transition moment $\boldsymbol{\mu}$ according to $A \propto \langle(\boldsymbol{\mu} \cdot \mathbf{E})^2\rangle$, knowledge of the electric field $\mathbf{E}$ can be combined with polarization-dependent absorbance measurements to probe molecular orientation of an adsorbed layer or a thin film. Using the Fresnel equations within a plane-wave approximation, we can calculate the electric field of the evanescent wave[15] as a function of the refractive indices, angle of incidence, polarization, and distance from the TIR surface. For S and P polarizations, the electric field direction and magnitude can be expressed as $\mathbf{E}_s/E_{\text{os}} = \Gamma_y y$ and $\mathbf{E}_p/E_{\text{op}} = \Gamma_x x + \Gamma_z z$, where E_{os} and E_{op} are the respective incident field amplitudes, Γ_x, Γ_y, and Γ_z are field enhancement (or modification) factors, and x, y, and z are unit vectors of the TIR surface coordinate system shown in the inset of Fig. 2. For $\theta_i = 45.0°$, the electric fields at a fused-silica–air interface ($z = 0$) were found to be $\mathbf{E}_s/E_{\text{os}} = 1.94y$ and $\mathbf{E}_p/E_{\text{op}} = 0.64x + 2.62z$ for S and P polarizations, respectively. To provide a simple demonstration of chemical detection, the adsorption of I_2 was examined, as in previous studies.[7,11] Figure 4 shows S- and P-polarized optical losses A_S and A_P as a function of time during exposure of the TIR surface to I_2 vapor, which was generated from solid I_2 at room temperature. The TIR surface was sealed to the I_2 cell with a Viton[16] O

ring as indicated in inset (a). Note that the S-polarized loss is considerably stronger than the P-polarized case, while the ratio $\rho = A_S/A_P$, remains essentially constant. If it is assumed that molecules are oriented with a well-defined polar angle Θ and randomly distributed in the azimuthal angle φ, which are defined in inset (b) of Fig. 4, then ρ is given by[18]

$$\rho(\Theta) = \frac{I_y}{I_x + 2I_z \cot \Theta}, \tag{3}$$

where $I_i = |E_i|^2$ with $i = x, y, z$. The results of Fig. 4 yield $\Theta \sim 88°$, suggesting that the transition moment of the surface-bound species lies in the plane of the surface. Alternatively, we can describe orientation by invoking a distribution function $N(\Theta,\varphi)$.[19] If $\rho(\Theta,\varphi)$ and $N(\Theta,\varphi)$ are expanded in spherical harmonics, $Y(\ell,m)$, a relationship between ρ and the expansion coefficients $d_{\ell m}$ of $N(\Theta,\varphi)$ can be derived. Assuming isotropy in φ we found this relationship to be given by

$$\rho = \frac{I_y(1 + d_{20})}{(I_x + I_z) + (2I_z - I_x)d_{20}}, \tag{4}$$

revealing that optical absorption measurements (in general) provide only a value for the ($\ell = 2$, $m = 0$) expansion coefficient d_{20}, which has been pointed out previously.[20] Additional information about the distribution function is therefore needed to fully elucidate molecular orientation, although depending on the precision of d_{20}, some differentiation between distributions may be possible.[21] Indeed many factors can complicate the interpretation of orientation measurements, including the existence of different adsorption sites or surface reactions. Multilayer adsorption could also complicate interpretation, although for adsorption of I_2 on silica the saturation coverage appears to be well below a full monolayer.[7,22] In addition, a contribution to the optical loss from the ambient bulk can be significant,[23] although for scan times of several minutes with a 10-Hz laser repetition rate, no gas-phase spectral structure was observed in these experiments over the limited bandwidth of the resonator.

4. Detection Limit

Based on a minimum detectable absorption of $(L_{abs})_{min} = 4 \times 10^{-7}$ and a room-temperature absorption cross section of $\sigma(540\ nm) \cong 2 \times 10^{-18}$ cm^2/molecule (Ref. 24) for I_2, a minimum detectable coverage can be estimated from $L_{abs} = 2\Gamma^2\sigma(\omega)N_s/\cos\theta_i$, where N_s is the surface density and Γ^2 is the intensity enhancement factor. Assuming $N_0 = 4.5 \times 10^{14}$ sites/cm^2 as the definition of one monolayer on the SiO_2 surface,[25] one can find a minimum detectable coverage of 0.004% of a monolayer. This rough estimate assumes that I_2 molecules lie flat on the SiO_2 surface so that the local electric field intensity is enhanced by $(\Gamma_S)^2 = (1.94)^2 \cong 3.8$. The gas-phase absorption cross section is also employed for reasons discussed previously.[7] One can realize an increase in sensitivity by working in spectral regions where bulk and coating losses are smaller or, to a certain degree, by reducing the size of the resonator. Between 520 nm and 1.5 μm, the bulk losses of fused silica decrease from $\sim 30 \times 10^{-6}$ cm^{-1} to $\sim 5 \times 10^{-7}$ cm^{-1} for selected material,[26] providing a significant reduction in $\mathcal{L}_0$. One can also expect improvements in sensitivity by employing single-mode excitation,[17] which should be facilitated by the monolithic design of the resonator. Single-mode excitation eliminates nonexponentially in the ringdown transient that accompanies multimode excitation, thereby improving decay-time measurement precision, if employed with low-noise detection and high-resolution digitization. The high sensitivity provided by EW-CRDS should enable a variety of novel fundamental studies, especially of surface processes. The technique also provides a new platform for chemical sensing when the analyte of interest can be detected at the surface. However, to fully elucidate any specific interaction, multiple techniques will likely be required to thoroughly characterize the surface conditions, analogous to studies on single crystals under ultrahigh vacuum.

This research was supported by the Environmental Management Science Program of the Department of Energy under contract DE-AI07-97ER62518.

References and Notes

1. A. O'Keefe and D. A. G. Deacon, "Cavity ring-down optical spectrometer for absorption measurements using pulsed laser sources," Rev. Sci. Instrum. **59,** 2544–2551 (1988).
2. M. D. Wheeler, S. M. Newman, A. J. Orr-Ewing, and M. N. R. Ashfold, "Cavity ring-down spectroscopy," J. Chem. Soc. Faraday Trans. **94**(3), 337–351 (1998).
3. K. W. Busch and M. A. Busch, eds., *Cavity-Ringdown Spectroscopy* (Oxford U. Press, New York, 1999).
4. D. Romanini and K. K. Lehmann, "Ring-down cavity absorption spectroscopy of the very weak HCN overtone bands with 6, 7, 8, stretching quanta," J. Chem. Phys. **99,** 6287–6301 (1993).
5. P. Zalicki and R. N. Zare, "Cavity ring-down spectroscopy for quantitative absorption measurements," J. Chem. Phys. **102,** 2708–2717 (1995).
6. M. Moretti, "Ultra-low loss measurements for high-performance optics," Laser Focus **23,** 22–26 (1987).
7. A. C. R. Pipino, J. W. Hudgens, and R. E. Huie, "Evanescent wave cavity ring-down spectroscopy for probing surface processes," Chem. Phys. Lett. **280,** 104–112 (1997).
8. A. C. R. Pipino, J. W. Hudgens, and R. E. Huie, "Evanescent wave cavity ring-down spectroscopy with a total-internal-reflection minicavity," Rev. Sci. Instrum. **68,** 2978–2989 (1997).
9. A. C. R. Pipino, "Evanescent wave cavity ring-down spectroscopy for ultrasensitive chemical detection," in *Advanced Sensors and Monitors for Process Industries and the Environment*, W. A. De Groot, ed., Proc. SPIE **3535,** 57–67 (1998).
10. R. Engeln, G. von Helden, A. J. A. van Roij, and G. Meijer, "Cavity ring-down spectroscopy on solid C_{60}," J. Chem. Phys. **110,** 2732–2733 (1999).
11. A. C. R. Pipino, "Ultrasensitive surface spectroscopy with a miniature optical resonator," Phys. Rev. Lett. **83,** 3093–3096 (1999).
12. A. E. Siegman, *Lasers* (University Science, Mill Valley, Calif., 1986).
13. N. J. Brown, "Preparation of ultrasmooth surfaces," Annu. Rev. Mater. Sci. **16,** 371–388 (1986).

14. S. Schiller, "Principles and applications of optical monolithic total internal reflection resonators," Ph.D. dissertation (Stanford University, Stanford, Calif., 1993).
15. N. J. Harrick, *Internal Reflection Spectroscopy* (Interscience, New York, 1967).
16. Identification of specific commercial products in this paper is provided to specify procedures completely. In no case does such identification imply recommendation or endorsement by the National Institute of Standards and Technology, nor does it imply that such products have necessarily been identified as the best available for the purpose.
17. R. D. van Zee, J. T. Hodges, and J. P. Looney, "Pulsed, single-mode cavity ringdown spectroscopy," Appl. Opt. **38,** 3951–3960 (1999).
18. D. M. Cropek and P. W. Bohn, "Surface molecular orientations determined by electronic linear dichroism in optical waveguide structures," J. Phys. Chem. **94,** 6452–6457 (1990).
19. I. M. Ward, "Determination of molecular orientation by spectroscopic methods," in *Characterization of Polymers in the Solid State 1: Part A, NMR and Other Spectroscopic Methods,* H. H. Kausch, H. G. Zachmann, and A. Apicella, eds., Volume 66 of Advances in Polymer Science (Springer-Verlag, Berlin, 1985).
20. N. L. Thompson, H. M. McConnell, and T. P. Burghardt, "Order in supported phospolipid monolayers detected by the dichroism of fluorescence excited by polarized evanescent illumination," Biophys. J. **46,** 739–747 (1984).
21. C.-P. Lafrance, A. Nabet, R. E. Prud'homme, and M. Pézolet, "On the relationship between the order parameter $[P_2(\cos\theta)]$ and the shape of orientation distributions," Can. J. Chem. **73,** 1497–1505 (1995).
22. G. Kortum and H. Koffer, "Diffuse reflexionsspektren von absorbiertem jod," Ber. Bunsenges. Phys. Chem. **67,** 67–75 (1963).
23. A. Charvat, S. A. Kovalenko, and B. Abel, "Attenuated total internal reflection spectroscopy with an intracavity laser absorption spectrometer," Spectrochim. Acta Part A **55,** 1553–1567 (1999).
24. J. G. Calvert and J. N. Pitts, Jr., *Photochemistry* (Wiley, New York, 1967).
25. R. K. Iler, *Chemistry of Silica* (Wiley, New York, 1979).
26. I. D. Aggarwal and G. Lu, eds., *Fluoride Glass Fiber Optics* (Academic, Boston, Mass., 1991).